SCIENTIFIC ARTICLE

Mechanism of Methylprednisolone-Induced Primary Cilia Formation Disorder and Autophagy in Osteoblasts

Zhen-qun Zhao, MD[1,2], Wan-lin Liu, MD[2], Shi-bing Guo, MD[3], Rui Bai, MD[2], Jing-long Yan, MD[1]

[1]Orthopedics Department, Second Affiliated Hospital of Harbin Medical University, Harbin and [2]Pediatric Orthopedics Department and [3]Bone Tumor Department, Second Affiliated Hospital of Inner Mongolia Medical University, Inner Mongolia, China

Objective: To study the role of primary cilia formation disorder and osteoblasts autophagy in the pathogenesis of steroid-induced avascular necrosis of the femoral head (SANFH).

Methods: Osteoblasts were isolated from rabbit bones and treated with 1 μM Methylprednisolone for 0, 12, 24, 48, and 72 h. The Beclin1, MAP1LC3, Atg-5, Atg-12, IFT20 and OFD1 mRNAs and proteins were detected by PCR and Western blotting, and their correlation was statistically analyzed. The lengths of osteoblast cilia were measured under a laser confocal microscope, and the autophagy flux was tracked by transfecting the osteoblasts with GFP-RFP-LC3 lentivirus.

Results: Methylprednisolone significantly upregulated Beclin1, MAP1LC3, Atg-5, Atg-12 and OFD1 mRNAs and proteins in a time-dependent manner, and decreased that of IFT20 ($P < 0.05$). In addition, the autophagy flux in the osteoblasts also increased and the ciliary length decreased in a time-dependent manner after Methylprednisolone treatment. The length of the cilia were 5.46 ± 0.11 um at 0 h, 4.08 ± 0.09 um at 12 h, 3.07 ± 0.07 um at 24 h, 2.31 ± 0.10 um at 48 h, and finally 1.15 ± 0.04 um at 72 h. Methylprednisolone treatment also affects primary cilium numbers in cultures, for 0 to 72 h. The autophagy regulatory genes, Beclin1, MAP1LC3, Atg-5 and Atg-12, were found to be negatively correlated with IFT20, with an average correlation coefficient of −0.81. A negative correlation was also found between OFD1 and IFT20, with an average correlation coefficient of −0.53.

Conclusion: Methylprednisolone inhibits primary cilia formation and promotes autophagy, which could be the pathological basis of SANFH. The exact regulatory mechanism needs to be further studied *in vivo*.

Key words: Autophagy; Methylprednisolone; Osteoblasts; Osteonecrosis; Primary cilia

Introduction

Osteonecrosis of the femoral head affects 20 mn people worldwide, with more than 200,000 cases diagnosed annually in China[1,2]. A multicenter review of 6395 patients with osteonecrosis of the femoral head in China found that 24.1% of the cases, especially those without trauma, were steroid induced[2]. In addition, steroid-induced avascular necrosis of the femoral head (SANFH) frequently occurs in young and middle-aged people, and is associated with a high risk of disability since it involves bilateral femoral heads. Interestingly, numerous cases of SANFH emerged after SARS in 2003[3,4], although the pathological basis remains unknown, thereby limiting prevention and treatment.

The loss of cartilage cells, osteocyte, and osteoblasts is hypothesized to drive SANFH[5,6], although the type of cell death is not completely clear. Autophagy is an auto-catabolic recycling process of eukaryotic cells that is frequently dysregulated in cancer, inflammatory diseases, autoimmune

Address for correspondence Jing-long Yan, MD, Orthopedics Department, Second Affiliated Hospital of Harbin Medical University, NO.148, Health Road, Nangang District, Harbin, China 150081 Tel: 0451-86605222; Fax:+8604 716351329; Email: 852495257@qq.com

Grant Sources: This work was supported by the National Natural Science Foundation of China (No. 81760391, 81560349, 81460331).
Received 23 September 2019; accepted 20 January 2020

Orthopaedic Surgery

diseases, aging, etc[7–10]. Our preliminary results show that SANFH is associated with autophagy, and the autophagy-related Beclin 1 and microtubule-associated protein 1 light chain 3 (MAP1LC3) are upregulated in osteoblasts[11]. Primary cilia are sensitive cellular antennae that sense and transmit external signals[12], and coordinate the responsive mechanisms[13]. Recent studies show that the formation of primary cilia depends on autophagy[14]. The intraflagellar transport 20 (IFT20) protein which regulates ciliary formation and length[15,16] is upregulated during starvation or lysosomal inhibition, and its knockdown during autophagy inhibits cilia formation[17]. IFT20 also recruits non-ciliary proteins to the plasma membrane, which is the site of autophagosome formation. Furthermore, autophagy is significantly decreased when ciliary formation is disrupted, which is the basis of ciliated disease[18]. The oral facial digital syndrome-1 (OFD1) is a centrosome satellite protein that suppresses cilia formation, and its autophagic degradation promotes the biosynthesis of primary cilia[19,20].

It is not clear at present whether primary cilia growth is related to avascular necrosis of the femoral head, or whether osteoblast autophagy affects primary cilia formation during local ischemia and hypoxia of the femoral head. To this end, we investigated the relationship between osteoblast autophagy and primary cilia formation in the presence of steroids. The purpose of this study is to: (i) determine whether primary ciliary formation disorder is associated with SANFH; (ii) determine whether osteoblast autophagy is associated with SANFH; and (iii) examine the relationship between primary cilia formation disorder and autophagy in osteoblasts under the action of Methylprednisolone.

Materials

Osteoblast

Twenty white rabbits from New Zealand aged 8 weeks and weighing 1.5 ± 0.2 kg (Jiangsu Yizheng Biotechnology Co. Ltd., Nanjing. China, Certificate No. SCXK [Su] 20160005) were raised in single cages exposed to natural light. The animal experiments conducted were in accordance with the 2009 "Ethical issues in animal experimentation," and approved by the Ethics Reviewing Council of Second Affiliated Hospital of Inner Mongolia Medical University (NO.YKD2016143, Inner Mongolia, China). The rabbits were anesthetized with intravenous injection of pentobarbital sodium (Sigma, Shanghai, China) into their ears. After swabbing the legs with alcohol (Nanjing Shengxing Biology, Nanjing, China), the animals were dissected and their femurs were removed. The bones were rinsed with sterile PBS (Nanjing Shengxing Biology, SN331, Nanjing, China), cut into small pieces, and washed once with DMEM (Hyclone, Shandong, China). The extraneous tissues were sequentially digested with 0.25% trypsin (Hyclone, Shandong, China) and 1 mg/mL collagenase I (Solarbio, C8140, Shanghai, China) for 20 min each at 37°C, and removed by centrifuging at 1000 rpm for 5 min. The marrow was flushed out of the cleaned bones with DMEM supplemented with 15% serum (Hyclone, Shandong, China), and incubated at 37°C with the medium replaced every 3 days. Once the cells were 50% confluent, the medium was replaced with DMEM containing 10% FBS and 1% penicillin + streptomycin (Hyclone, Shandong, China). The cells were harvested once they grew to 80%–90% confluency using 0.25% trypsin as per standard protocol.

Real-Time Polymerase Chain Reaction

Total RNA and miRNAs were isolated from the osteoblasts using TRIzol Reagent (Invitrogen, Shanghai, China) and miRNA Extraction Kit (Ribobio, Guangzhou, China) respectively, and the former was reverse transcribed to cDNA using PrimeScript RT Reagent Kit (TaKaRa, Dalian, China). RT-PCR was performed using SYBR Premix Ex Taq and SYBR Green I PCR Kit (TaKaRa, Dalian, China) in the ABI Step One Plus Real-Time PCR System (Applied Biosystems; Thermo Fisher Scientific, Shanghai, China) with the following cycling conditions: initial denaturation for 5 min at 95°C and 40 cycles of denaturation at 95°C for 10 s, followed by annealing and extension at 60°C for 34 s. All steps were performed as per the manufacturers' instructions, and the experiment was repeated thrice. The primer sequences were as follows: Beclin1—forward 5′-GTACAGGATGGATGTGG AGAAAG-3′ and reverse 5′-TGTCCACTGTTCCTCAGAA TTG-3′; LC3—forward 5′-AGAACGATACAAGGGTGAGA AG-3′ and reverse 5′-GGCGCCTCCTGATGATTT-3′; Atg5—forward 5′-TGAAAGGGAAGCAGAACCATAC-3′ and reverse 5′-TCAGTGGTGTGCCTTCATATTC-3′; Atg12—forward 5′-CTGGCGAC ACCAAGAAGAAA-3′ and reverse 5′-GGATGGTTCTTGTTCGCTCTAC-3′; IFT20—forward 5′-GACCATAGAGCTCAAGGAAGAG-3′ and reverse 5′-GCAAGTTGGTCAACGAGTTC-3′; OFD1—forward 5′-TCAAAGACACGAGCGATGAC-3′ and reverse 5′-CTGTCCTTCATCCTTGCTAAGT-3′; GAPDH—forward 5′-GCGTGAACCACGAGAAGTAT-3′ and reverse 5′-CCT CCACAATGCCGAAGT-3′.

Western Blotting

Total protein was extracted by homogenizing each sample with 100 μL RIPA lysis solution (Aladdin Biochemistry, Shanghai, China) on ice for 30 min. The lysates were centrifuged at 12,000 rpm for 5 min at 4°C, and the protein content of the supernatants were measured using the BCA assay kit (Biyuntian, Shanghai, China). Equal amounts of protein per sample were separated by SDS-PAGE using the Mini-PROTEAN 3 system (Bio-Rad, Shanghai, China), and the protein bands were transferred to PVDF membranes using the Trans-Blot SD wet transfer system (Bio-Rad, Shanghai, China). After blocking the membranes with 5% skim milk powder in TBST buffer (Shanghai, China) at room temperature for 1 h, they were incubated overnight with the

primary antibodies in TBST solution containing 5% BSA (Aladdin Biochemistry, Shanghai, China) at 4°C. The blots were washed thrice with TBST at room temperature, and then incubated with the secondary antibody at room temperature for 2 h. After washing thrice with TBST, the blots were developed using the Tanon chemiluminescence sensor system (Tanon, Shanghai, China). GAPDH was used as the loading control.

Autophagy Flux Analysis

Osteoblasts were seeded in 3.5 cm glass bottom petri dishes at the density of 2×10^6 cells/dish, and allowed to adhere overnight. The complete medium was replaced with serum-free medium, and the cells were infected with GFP-RFP-LC3 lentivirus (Gima Pharmaceutical Co. Ltd., Shanghai, China) at the MOI of 1:50. After 6 h, the medium was removed and fresh complete medium was added. The cells were cultured for 48 h, and transduction efficiency was observed under a fluorescence microscope. The stably transduced cells were treated with 1 μM Methylprednisolone for 0, 12, 24, 48, or 72 h, and fixed with 4% paraformaldehyde at room temperature for 10 min. The green and red fluorescence respectively indicating autophagosome and autophagolysosome formation were observed by laser confocal microscope.

Immunofluorescence

Glass slides were pre-coated with 0.1% agar either overnight at room temperature or at 37°C for 2 h, and sterilized under ultraviolet light for 30 min. The osteoblasts were seeded onto the slides and, after overnight culture, treated with 1 μM Methylprednisolone followed by serum starvation (0.5% FBS) for 24 h to induce ciliation. The cells were washed thrice with PBS and fixed with 4% paraformaldehyde for 15 min at 4°C. After washing again with PBS three times, the cells were permeabilized and blocked with 3% BSA/0.3% NP-40 for 30 min with constant shaking at room temperature. The cells were incubated overnight with the primary antibody against α-tubulin (1:1000) at 4°C, washed thrice with 0.1% PBS-Tween, followed by the secondary antibody (1:200) at room temperature for 1 h. After washing thrice with 0.1% PBST, the cells were counterstained with DAPI, sealed, and observed under a laser confocal microscope. The images were analyzed using the Zen software (Zeiss, Shanghai, China).

Electron Microscopy

The methylprednisolone-treated cells were fixed overnight in 2.5% glutaraldehyde at 4°C, followed by 1% osmium tetroxide for 1 h at room temperature. The fixed cells were immobilized in 10% gelatin and fixed again with glutaraldehyde for 1 h at 4°C. After dehydrating across an ethanol gradient (30%, 50%, 70%, 90%, 95%, 100%, 100%), the samples were immersed in epoxy resin, cut into ultrathin sections with a Leica UC6 (Leica, EM UC6, Germany), and observed under a transmission electron microscope (TEM) (JEM1011, Japan).

Statistical Analysis

The results were presented as mean ± standard deviation of three independent experiments. All statistical analyses were conducted using SPSS 20.0 software (IBM, Armonk, NY, USA). Beclin1, MAP1LC3, Atg-5, Atg-12 and OFD1 mRNAs and proteins, numbers and length of primary cilium were compared by one-way analysis of variance (ANOVA), followed by LSD test. The correlation between autophagy gene expression and cilia length was analyzed using linear

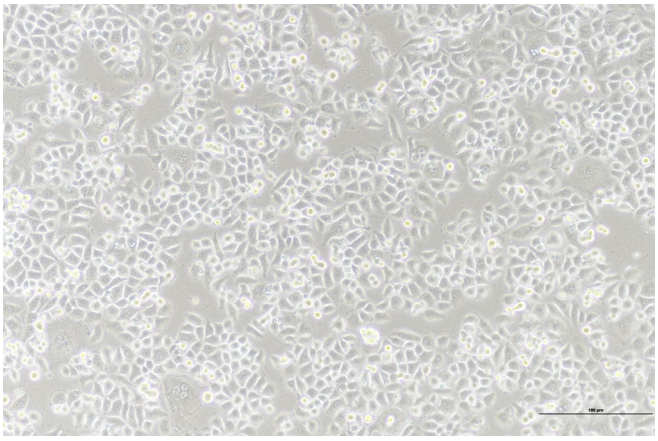

Fig. 1 White light images of osteoblasts showing large and round nucleus, high amounts of cytoplasm and scale-like surface.

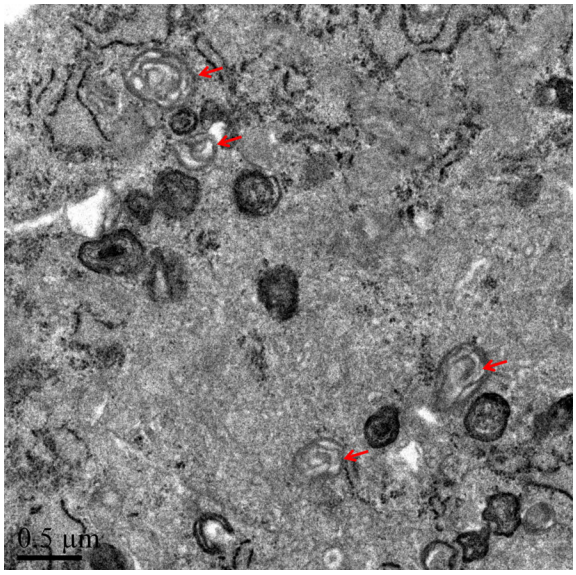

Fig. 2 Electron micrographs showing autophagosomes (red arrow) in the osteoblasts after Methylprednisolone treatment.

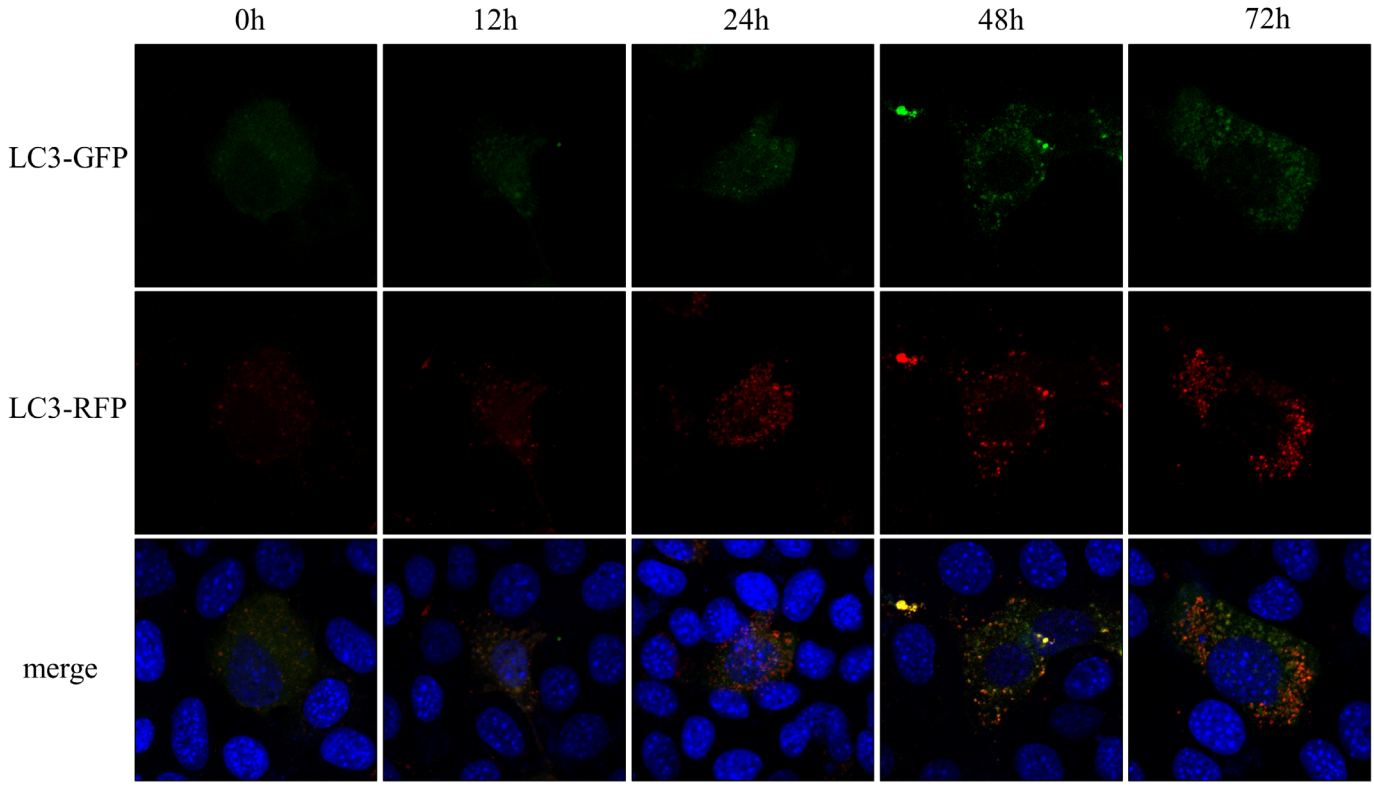

Fig. 3 Fluorescence images showing the autophagy flux in the methylprednisolone-treated osteoblasts. A gradually increasing number of RFP-GFP-LC3 double-label positive staining cells were found from 0 to 72 h.

correlation analysis. *P* values <0.05 were considered statistically significant.

Results

Osteoblast Morphology

Osteoblasts are arranged in a monolayer, and the cell bodies are either cubic or dwarf columnar in shape. There are many small processes on the cell surface, which form a gap junction with adjacent osteoblasts or osteocyte. The nucleus is large and round, the cell culture is scale-like, the cytoplasm is rich, and pseudopods are present (Fig. 1).

Osteoblast Autophagosomes

Under an electron microscope, the autophagosome appears grayish white, and there is a double-layer or multi-layer membrane-like structure that has a tendency to wrap around the cytoplasm, and the vacuole-like structure containing cytoplasmic components is wrapped by a double-layer or multi-layer membrane (with an average diameter of about 500 nm). The monolayer film structure surrounds broken and degraded components (Fig. 2). After Methylprednisolone was added to osteoblasts, during an extension of time (0 to 72 h), the number of autophagosomes gradually increased in the osteoblasts, as seen under an electron microscopy, but this increase could not be statistically analyzed.

The Promoting Effects of Methylprednisolone in the Autophagy of Osteoblasts

Autophagy Flow

After the merge of red and green fluorescence, the visible yellow spots were autophagosomes. The red spots indicate autophagy lysosomes. If the phagosome and lysosome can fuse, then red fluorescence increases, compared with that of the yellow fluorescence. However, when there is an

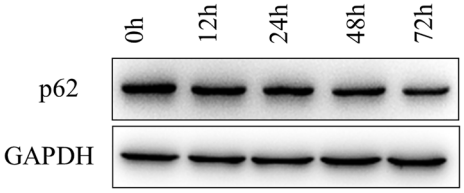

Fig. 4 Autophagic flux was analyzed by assessing p62 levels following treatment at the different time points, antivirus does not affect autophagy flow results.

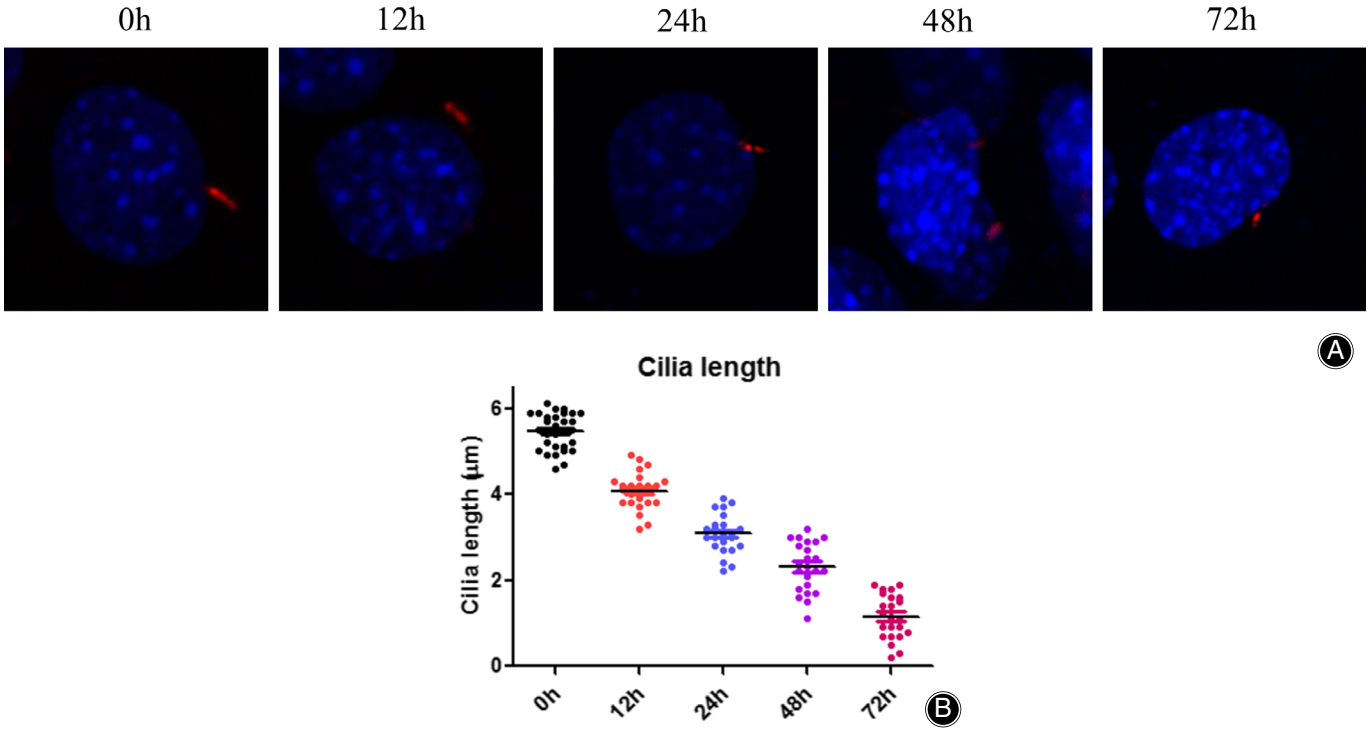

Fig. 5 Primary ciliary length after methylprednisolone treatment for varying durations, the primary cilia of the osteoblasts gradually shortened along with an increase in time.

autophagy block downstream, phagosomes and lysosomes cannot fuse as normal, and only a yellow fluorescence is mainly visible. As shown in Fig. 3, after treatment with Methylprednisolone for 12 to 72 h, compared with the control and the 0 h group, a gradually increasing number of RFP-GFP-LC3 double-label positive staining cells were found. For 0 to 72 h, the average positive staining cells were 3%, 8%, 10%, 21%, and 35%.

P62 Levels

As shown in Fig. 4, to prevent lentivirus from affecting autophagy flow results, autophagic flux was also analyzed by assessing p62 levels following treatment at the different time points. For 0 to 72 h, the average gray value of p62 was 1.56, 1.45, 1.26, 0.95, and 0.63, respectively. Compared with 0 h from 12 to 72 h, the *P* values were 0.081, 0.005, 0.0003, and 0.0001, respectively.

The Inhibition Effects of Methylprednisolone Primary Cilia Length and Numbers

Primary Cilia Length

When Methylprednisolone was added to the osteoblasts, the primary cilia of the osteoblasts gradually shortened along with an increase in time (Fig. 5). The length of the cilia were 5.46 ± 0.11 um at 0 h, 4.08 ± 0.09 um at 12 h, 3.07 ± 0.07 um at 24 h, 2.31 ± 0.10 um at 48 h, and finally 1.15 ± 0.04 um at 72 h. The ANOVA analysis found significant differences among the four groups ($P = 0.003$), while the LSD test analysis also found significant difference within groups ($P = 0.006$). Compared with 0 h, the length of primary cilia from 12 to 72 h was 74.73%, 56.23%, and 42.31%, respectively.

Primary Cilia Numbers

Methylprednisolone treatment also affects primary cilium numbers in cultures (Fig. 6). Each group counted 200 cells

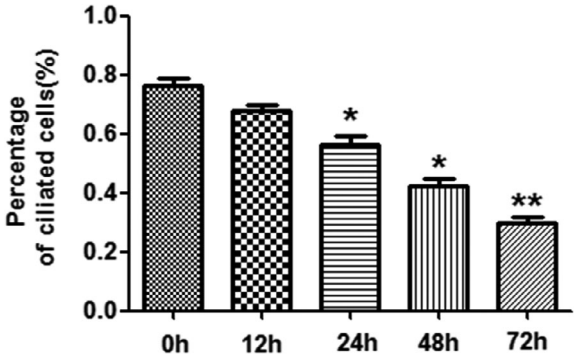

Fig. 6 Primary ciliary numbers after Methylprednisolone treatment for varying durations.*$P < 0.05$ and **$P < 0.01$ *vs* 0 h.

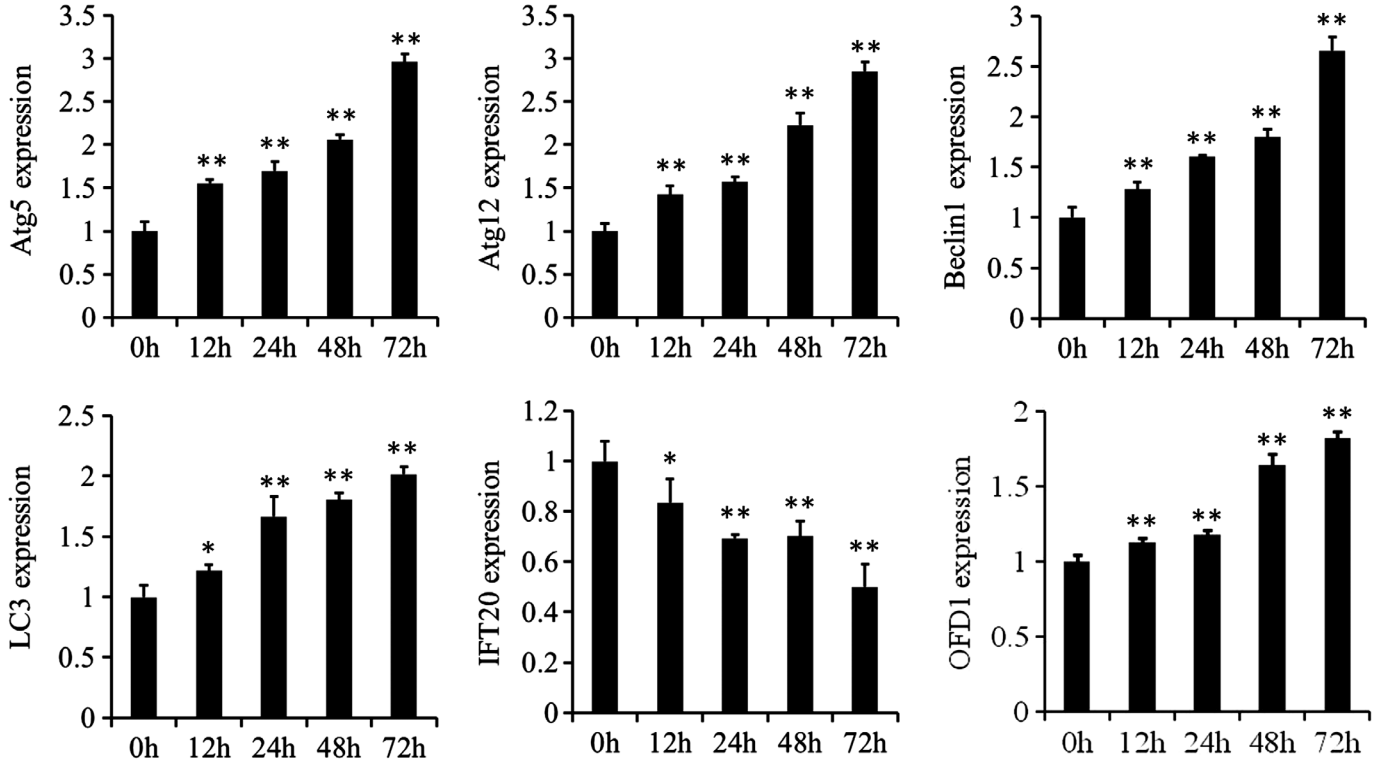

Fig. 7 Methylprednisolone regulates autophagy and ciliary genes. Time-dependent changes in the expression levels of LC3, Beclin1, Atg5, Atg12, OFD1 and IFT20 mRNAs in the methylprednisolone-treated osteoblasts. *$P < 0.05$ and **$P < 0.01$ *vs*. control group.

and repeated three times. For 0 to 72 h, the average primary cilium numbers was 162, 142, 124, 92, and 52, respectively.

Effects of Methylprednisolone in Autophagy Genes and Primary Cilia in Osteoblasts

The results of the PCR show that in the key autophany genes, Beclin1, MAP1LC3, Atg-5 and Atg-12, and the primary cilia regulatory gene, OFD1, mRNA levels gradually increased at 0, 12, 24, 48, and 72 h after Methylprednisolone treatment, while in the primary cilia regulatory gene, IFT20, mRNA levels gradually decreased. Significant differences were found between levels of Beclin1, MAP1LC3, Atg-5, Atg-12, OFD1 and IFT20 at 12, 24, 48, and 72 h after Methylprednisolone treatment, compared with the GAPDH control group ($P < 0.01$) (Fig. 7–9).

Effects of Methylprednisolone in Autophagy Genes and Primary Cilia mRNA Regulation of Osteoblasts

The autophagy regulatory genes Beclin1, MAP1LC3, Atg-5 and Atg-12 were found to be positively correlated with OFD1, with an average correlation coefficient of 0.76. The autophagy regulatory genes, Beclin1, MAP1LC3, Atg-5 and Atg-12, were found to be negatively correlated with IFT20, with an average correlation coefficient of −0.81. A negative correlation was also found between OFD1 and IFT20, with an average correlation coefficient of −0.53.

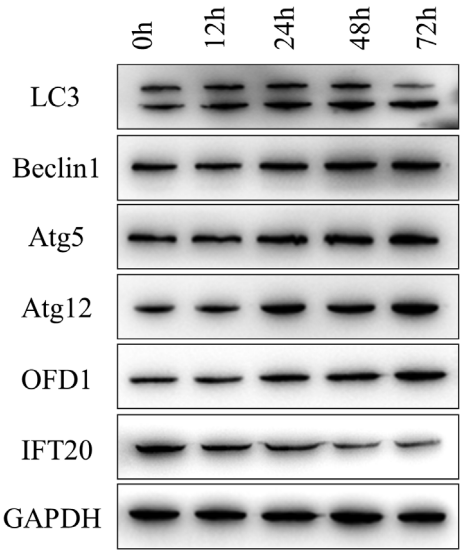

Fig. 8 Immunoblots showing time-dependent changes in the expression levels of autophagy and ciliary associated proteins in the osteoblasts treated with Methylprednisolone.

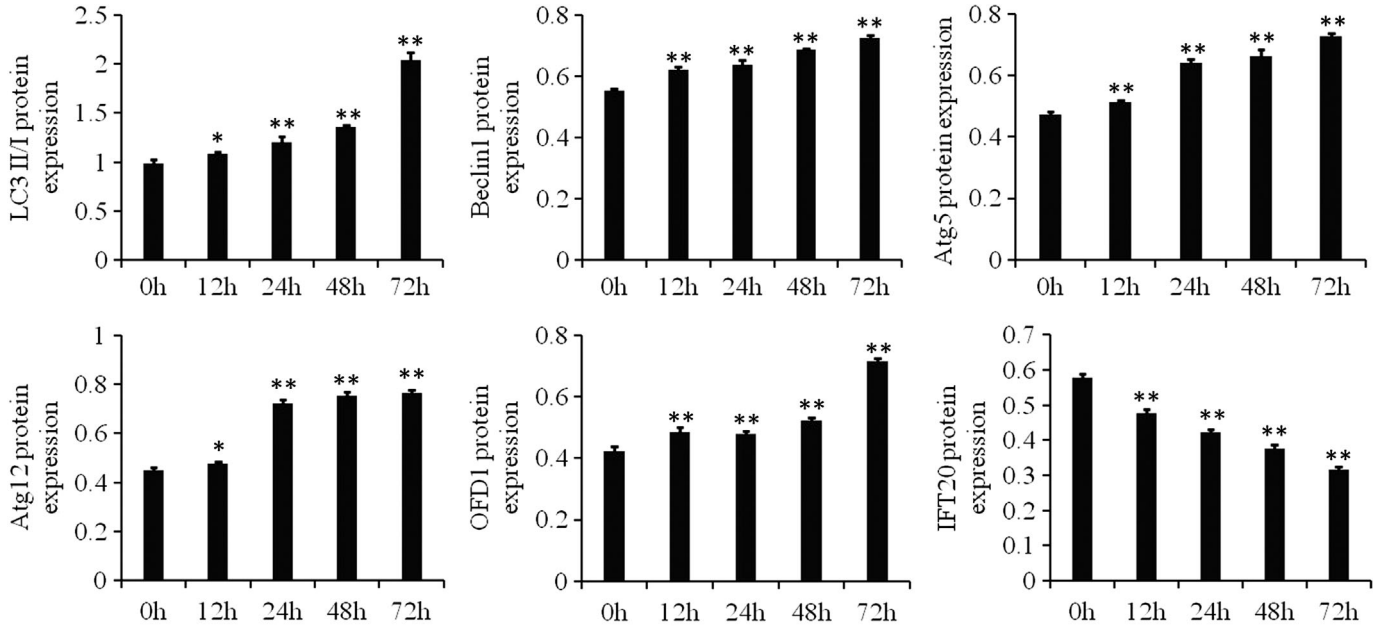

Fig. 9 Bar graphs comparing the expression of autophagy and ciliary formation proteins at the different time points of Methylprednisolone treatment. $^{*}P < 0.05$.

Discussion

Long-term use of glucocorticoids decreases bone mineral density, reduces the number of osteoblasts and osteoclasts, and prolongs osteoclast survival, eventually resulting in an imbalance between bone resorption and remodeling[21]. However, only 15% to 20% of the osteocytes in the femoral head were apoptotic in the mouse model of SANFH[22], indicating other pathological mechanisms. Lane *et al.* found that glucocorticoids increase the gap between osteocytes, which results in the loss of minerals and disrupts bone metabolism independent of apoptosis[23]. Xia *et al.* first reported that dexamethasone increased autophagy in osteoblasts, which was verified in the primary osteoblasts isolated from prednisolone-treated mice[24]. In the current study, we detected increased Beclin 1 expression in the femoral head tissues of a rabbit model of SANFH, indicating that autophagy is also a pathological basis of SANFH. This is consistent with a previous study which showed that inhibition of autophagy by 3-MA retarded SANFH development *in vivo*[25]. Under physiological conditions with functioning osteoblasts, necrosis of the femoral head is repaired naturally. Therefore, glucocorticoids likely inhibit osteoblast function to aggravate SANFH. Luo *et al.* reported that Methylprednisolone increased autophagy in bone cells in a model of SANFH in a dose-dependent manner, which also affects the interaction between osteoblasts and osteoclasts[6]. We found that Methylprednisolone upregulated the key autophagy genes in the osteoblasts, along with increasing autophagy flux.

IFT20 and OFD1 regulate primary cilia formation and length in various cell types[15–17,19,20]. Delaine-Smith *et al.* found that the primary cilia of osteoblasts responded to fluid shear stress and interstitial flow-induced deposition of calcium in the bone[26], which was confirmed by a later study[27]. We found that Methylprednisolone decreased the cilia length of osteoblasts by upregulating OFD1 and downregulating IFT20. This is consistent with the study of Tang *et al.*, which showed that autophagy promoted cilia formation through selective degradation of OFD1. While LC3 specifically targeted OFD1 to the autophagy corpuscles for degradation, its centrosomal and basal parts were retained[28]. Pampliega *et al.* found that IFT20 was necessary for cilia formation and assembly, and was also degraded by autophagy to inhibit ciliation[29]. Taking both studies together, selective elimination of IFT20 during cell growth and proliferation hinders cilia formation while degradation of OFD1 during growth arrest promotes cilia formation. In this study, glucocorticoids gradually upregulated OFD1 and decreased IFT20 in the osteoblasts. We concluded, therefore, that glucocorticoids block the signal transduction of osteoblasts by selectively eliminating IFT20 during cell growth and proliferation.

Recent studies have shown a regulatory role of cilia in autophagy[30]. Wang *et al.* analyzed two renal cell lines with short and long cilia, and found that the former were activated by mTOR and resistant to autophagy[31]. In addition, Orhon *et al.* induced autophagy through the mechanical stress of fluid flow, which was regulated by the signal transduction pathway of primary cilia[32,33]. Jang *et al.* found that inhibition of cilia-mediated autophagy partly hindered neuroectoderm differentiation, underscoring the functional role of cilia in autophagy regulation[34]. Taken together, autophagy

and cilia formation regulate each other, but the exact regulatory mechanism needs to be further studied. We found that the autophagy genes were positively correlated with OFD1 and negatively correlated with IFT20.

Our study still has limitations. This study is an *in vitro* experiment and we cannot confirm whether the *in vivo* experiment has the same pathological process. This study is the effect of Methylprednisolone on osteoblasts and we cannot confirm whether other glucocorticoid have similar effects. Finally, this study can only confirm the relationship between osteoblast autophagy and primary cilia formation disorder in SANFH, but the exact regulatory mechanism is still unclear. To the best of our knowledge, this is the first study reporting that excessive autophagy and primary cilia disruption are potential mechanisms underlying osteoblast loss in SANFH. To summarize, glucocorticoid disturbs primary cilia formation in osteoblasts, which likely affects osteogenesis and destroys the dynamic balance between bone generation and resorption, eventually leading to SAFH.

References

1. Mont A, Zywiel G, Marker R, McGrath M, Delanois R. The natural history of untreated asymptomatic osteonecrosis of the femoral head: a systematic literature review. J Bone Joint Surg Am, 2010, 92: 2165–2170.
2. Cui L, Zhuang Q, Lin J, *et al*. Multicentric epidemiologic study on six thousand three hundred and ninety-five cases of femoral head osteonecrosis in China. Int Orthop, 2016, 40: 267–276.
3. Guo K, Zhao F, Guo Y, Li FL, Zhu L, Zheng W. The influence of age, gender and treatment with steroids on the incidence of osteonecrosis of the femoral head during the management of severe acute respiratory syndrome: a retrospective study. Bone Joint J, 2014, 96-B: 259–262.
4. Liu T, Ma J, Su B, Wang H, Wang Q, Ma X. A 12-year follow-up study of combined treatment of post-severe acute respiratory syndrome patients with femoral head necrosis. Ther Clin Risk Manag, 2017, 13: 1449–1454.
5. Kubo T, Ueshima K, Saito M, Ishida M, Arai Y, Fujiwara H. Clinical and basic research on steroid-induced osteonecrosis of the femoral head in Japan. J Orthop Sci, 2016, 21: 407–413.
6. Luo P, Gao F, Han J, Sun W, Li Z. The role of autophagy in steroid necrosis of the femoral head: a comprehensive research review. Int Orthop, 2018, 42: 1747–1753.
7. Zhao Y, Wang Z, Zhang W, Sun W, Li Z. MicroRNAs play an essential role in autophagy regulation in various disease phenotypes. Biofactors, 2019, 45: 844–856.
8. Mehto S, Jena K, Nath P, *et al*. The Crohn's disease risk factor IRGM limits NLRP3 inflammasome activation by impeding its assembly and by mediating its selective autophagy. Mol Cell, 2019, 73: 429–445.
9. Robin M, Issa R, Santos C, *et al*. Drosophila p53 integrates the antagonism between autophagy and apoptosis in response to stress. Autophagy, 2019, 15: 771–784.
10. Wang P, Zhao Z, Guo S, *et al*. Roles of microRNA-22 in suppressing proliferation and promoting sensitivity of osteosarcoma cells via metadherin-mediated autophagy. Orthop Surg, 2019, 11: 285–293.
11. Liu W, Zhao Z, Na Y, Meng C, Wang J, Bai R. Dexamethasone-induced production of reactive oxygen species promotes apoptosis via endoplasmic reticulum stress and autophagy in MC3T3-E1 cells. Int J Mol Med, 2018, 41: 2028–2036.
12. Park SM, Jang HJ, Lee JH. Roles of primary cilia in the developing brain. Front Cell Neurosci, 2019, 13: 218.
13. Ko JY, Lee EJ, Park JH. Interplay between primary cilia and autophagy and its controversial roles in cancer. Biomol Ther (Seoul), 2019, 27: 337–341.
14. Lee J, Yi S, Kang YE, *et al*. Defective ciliogenesis in thyroid hürthle cell tumors is associated with increased autophagy. Oncotarget, 2016, 7: 79117–79130.
15. Huang Q, Liu H, Zeng J, *et al*. COP9 signalosome complex subunit 5, an IFT20 binding partner, is essential to maintain male germ cell survival and acrosome biogenesis. Biol Reprod, 2019: ioz154. https://doi.org/10.1093/biolre/ioz154.
16. Finetti F, Cassioli C, Cianfanelli V, *et al*. The intraflagellar transport protein IFT20 controls lysosome biogenesis by regulating the post-Golgi transport of acid hydrolases. Cell Death Differ, 2020, 27: 310–328.
17. Ko JY, Yoo KH, Song SA, *et al*. Inactivation of max-interacting protein 1 induces renal cilia disassembly through reduction in levels of intraflagellar transport 20 in polycystic kidney. J Biol Chem, 2013, 288: 6488–6497.
18. Yuan X, Yang S. Cilia/Ift protein and motor -related bone diseases and mouse models. Front Biosci (Landmark Ed), 2015, 20: 515–555.
19. Tang Z, Zhu M, Zhong Q. Self-eating to remove cilia roadblock. Autophagy, 2014, 10: 379–381.
20. Lee YL, Santé J, Comerci CJ, *et al*. Cby1 promotes Ahi1 recruitment to a ring-shaped domain at the centriole-cilium interface and facilitates proper cilium formation and function. Mol Biol Cell, 2014, 25: 2919–2933.
21. Canalis E. Mechanisms of glucocorticoid action in bone. Curr Osteoporos Rep, 2005, 3: 98–102.
22. Weinstein R, Jilka R, Parfitt A, Manolagas S. Inhibition of osteoblastogenesis and promotion of apoptosis of osteoblasts and osteocytes by glucocorticoids. Potential mechanisms of their deleterious effects on bone. J Clin Invest, 1998, 102: 274–282.
23. Lane N, Yao W, Balooch M, *et al*. Glucocorticoid-treated mice have localized changes in trabecular bone material properties and osteocyte lacunar size that are not observed in placebo-treated or estrogen-deficient mice. J Bone Miner Res, 2006, 21: 466–476.
24. Xia X, Kar R, Gluhak-Heinrich J, *et al*. Glucocorticoid-induced autophagy in osteocytes. J Bone Miner Res, 2010, 25: 2479–2488.
25. Sun L, Liu W, Na R, Zhao Z. 3-Methyladenine regulating autophagy gene Beclin1 can alleviate the occurrence and development of steroid-induced avascular necrosis of the femoral head. Zhong Guo Zu Zhi Gong Cheng Yan Jiu, 2019, 40: 2391–2396.
26. Delaine-Smith RM, Sittichokechaiwut A, Reilly GC. Primary cilia respond to fluid shear stress and mediate flow-induced calcium deposition in osteoblasts. FASEB J, 2014, 28: 430–439.
27. Moore E, Zhu Y, Ryu HS, Jacobs C. Correction to: periosteal progenitors contribute to load-induced bone formation in adult mice and require primary cilia to sense mechanical stimulation. Stem Cell Res Ther, 2018, 9: 229.
28. Tang Z, Lin M, Stowe T, *et al*. Autophagy promotes primary ciliogenesis by removing OFD1 from centriolar satellites. Nature, 2013, 502: 254–257.
29. Pampliega O, Orhon I, Patel B, *et al*. Functional interaction between autophagy and ciliogenesis. Nature, 2013, 502: 194–200.
30. Orhon I, Dupont N, Pampliega O, Cuervo A, Codogno P. Autophagy and regulation of cilia function and assembly. Cell Death Differ, 2015, 22: 389–397.
31. Wang S, Livingston J, Su Y, Dong Z. Reciprocal regulation of cilia and autophagy via the MTOR and proteasome pathways. Autophagy, 2015, 11: 607–616.
32. Orhon I, Dupont N, Codogno P. Primary cilium and autophagy: the avengers of cell-size regulation. Autophagy, 2016, 12: 2258–2259.
33. Orhon I, Dupont N, Zaidan M, *et al*. Primary-cilium-dependent autophagy controls epithelial cell volume in response to fluid flow. Nat Cell Biol, 2016, 18: 657–667.
34. Jang J, Wang Y, Lalli M, *et al*. Primary cilium-autophagy-Nrf2 (PAN) axis activation commits human embryonic stem cells to a neuroectoderm fate. Cell, 2016, 165: 410–420.